This paper describes objective technical results and analysis. Any subjective views or opinions that might be expressed in the paper do not necessarily represent the views of the U.S. Department of Energy or the United States Government.

SAND2019-4222J

MANUSCRIPT

Solubility Model for Ferrous Iron Hydroxide and Hibbingite in Sodium Chloride Solutions in the Presence of Ethylenediaminetetraacetate

Jay Je-Hun Jang*, Martin Nemer[1], Cassandra Marrs, Jandi Knox, Heather Burton

Sandia National Laboratories, Repository Performance, 4100 National Parks Highway, Carlsbad, New Mexico, 88220, U.S.A.

* Corresponding author, Email: jjang@sandia.gov

[1] Now at Sandia National Laboratories, Diagnostic Science and Engineering, Albuquerque, New Mexico, U.S.A.)

Keywords: solubility, ferrous iron, $Fe(OH)_2(s)$, $Fe_2Cl(OH)_3(s)$, Pitzer activity coefficient equation, brine, nuclear waste disposal, $EDTA^{-4}$, complexation

Sandia National Laboratories is a multimission laboratory managed and operated by National Technology & Engineering Solutions of Sandia, LLC, a wholly owned subsidiary of Honeywell International Inc., for the U.S. Department of Energy's National Nuclear Security Administration under contract DE-NA0003525.

ABSTRACT

A solubility model for ferrous iron hydroxide and hibbingite in sodium chloride solutions was extended, based on a series of experiments, to include the complexation of dissolved ferrous iron (Fe^{+2}) with ethylenediaminetetraacetate ($C_{10}H_{12}O_8N_2^{-4}$, $EDTA^{-4}$). Calculated ionic strength of solutions ranged 0.14 - 3.6 moles/kg of H_2O (molality), and total $EDTA^{-4}$ molality kept constant at 0.041(±0.005) moles/kg of H_2O. All experiments were prepared using crimp-to-seal glass bottles under ambient temperature and pressure inside gloveboxes with less than 1 ppm oxygen for the long term aging exceeding 500 days. The Pitzer activity coefficient equation was used to account for non-ideal interaction behaviors of aqueous species. Experiments were conducted under conditions close to the boundary of ferrous iron hydroxide and hibbingite at ≥ 0.75 NaCl moles/kg of H_2O. X-ray diffraction data corroborated the coexistence of ferrous iron hydroxide and hibbingite. No solids containing $EDTA^{-4}$ were observed. An Fe^{+2} - $EDTA^{-4}$ complex with a formation constant chosen in this study effectively suppressed the formation of an Am^{+3} - $EDTA^{-4}$ complex in an exemplary calculation.

INTRODUCTION

The Waste Isolation Pilot Plant (WIPP) is a deep underground repository developed by the U.S. Department of Energy (DOE) to permanently isolate defence-related transuranic (TRU) radioactive wastes. It is located within bedded salts of the Permian Salado Formation, which consists of interbedded halite (NaCl) and anhydrite ($CaSO_4$) layers overlaying the Castile Formation near Carlsbad, New Mexico, U.S.A. WIPP has been designed to take advantage of the properties of rock salts, e.g., low porosity and self-sealing. Substances containing ethylenediaminetetraacetate ($C_{10}H_{12}O_8N_2^{-4}$, $EDTA^{-4}$), also known as ethylenedinitrilotetraacetate, is inventoried in nuclear wastes that will be or have been disposed of at WIPP (Waste Isolation Pilot Plant) (van Soest, 2012). $EDTA^{-4}$ poses concerns because it can form soluble, hence mobile, aqueous complexes with various metallic cations, including actinides (Pokrovsky et al., 1998).

The iron (Fe) inventory at WIPP is due to the components within emplaced wastes, repository infrastructure, and the steel canisters that contain the waste for emplacement (van Soest, 2012). After the permanent closure of WIPP, a possible scenario includes consumption of lingering oxygen by microbial activity and then anoxic corrosion of metallic iron (Fe) in highly saline, corrosive brine. The products of the iron corrosion under oxygen-deficient conditions would be the dissolved and precipitated ferrous iron species, such as ferrous iron hydroxide ($Fe(OH)_2$(s), FIH) and hibbingite ($Fe_2Cl(OH)_3$(s), HIBB).

It is expected that Fe^{+2} will decrease the extent of the actinide - $EDTA^{-4}$ complexation by competitively forming Fe^{+2} - $EDTA^{-4}$ complexes. There are few published equilibrium constants at infinite dilution for the reaction

$$FeEDTA^{-2} = Fe^{+2} + EDTA^{-4}. \quad (1)$$

Morel and Hering (1993) lists -16.1 for a 10-based logarithm of the equilibrium constant for Reaction (1), logK($FeEDTA^{-2}$) hereafter, at zero ionic strength and 25 °C. For the same reaction, Martell and Smith (1974) reported logK($FeEDTA^{-2}$) = -14.27 at an ionic strength of 0.1 (the unit for ionic strength not given therein) and 25 °C. Clark and Martell (1988) reported logK($FeEDTA^{-2}$) = -14.94 for the same reaction without specifying the ionic strength used for their investigation.

In this work, a solubility model for FIH and HIBB is extended to include the complexation of Fe^{+2} and $EDTA^{-4}$ through measurements of the total dissolved concentration of ferrous iron in sodium chloride (NaCl) solutions at a fixed concentration of $EDTA^{-4}$ inside the anoxic gloveboxes at ambient temperature and pressure. We used logK($FeEDTA^{-2}$) = -16.1 (Morel and Hering, 1993) for data analysis because this is the only literature value that was extrapolated to zero ionic strength. The other pertinent equilibrium constants and activity coefficients were referenced from Kim et al. (2017).

MATERIALS AND METHODS

Anoxic gloveboxes filled with the oxygen-scrubbed argon or nitrogen were used to minimize oxidation of Fe^{+2} by oxygen during the experimentation. Oxygen concentration within the gloveboxes (Labconco and VAC) routinely read less than 1 ppm. The oxygen concentration readings reached up to 10 ppm when the vacuum chamber doors were operated to move supplies and samples into or out of the gloveboxes. Whenever the vacuum chamber door was operated, experimentation inside the gloveboxes resumed after at least one hour to ensure the oxygen concentration decreased well below the detection limit.

All experiments were prepared inside the gloveboxes using 50-mL plastic and glass serum bottles that can be sealed with rubber seals and aluminum crimps. Deionized (DI) water was purged by circulating the inert gas of the gloveboxes through the DI water for at least three hours to produce deoxygenated, deionized (DDI) water. Purging was performed when the oxygen level was the lowest possible. To prepare $Fe(OH)_2(s)$, 24.9 gram of $FeCl_2.4H_2O$ (Fisher®) was dissolved in ~100 mL DDI water, and 10.0 gram of NaOH (Fisher®) was dissolved in ~100 mL DDI water. NaOH solution was transferred to the $FeCl_2$ solution. Precipitation occurred instantly. The container of NaOH solution was repeatedly rinsed with DDI water and the rinsate was added to the mixture to ensure quantitative chemical transfer until the total volume reached 500 mL inside the glovebox. After at least a week of periodic shaking bottles, the solid in the suspension was collected on a paper filter (Whatmann 40) and dried inside the gloveboxes. $EDTA^{-4}$ was added in the form of $Na_2H_2EDTA.2H_2O$ (Fisher®). Initial pH was measured after all reagents were added. 500- and 1000-days aged solutions were sampled for total dissolved concentration measurements of Fe^{+2}, Na^+, Cl^- and $EDTA^{-4}$.

An Inductively Coupled Plasma - Atomic Emission Spectrophotometer (ICP-AES, Perkin Elmer®, OPTIMA 3000 Dual View) was implemented to measure the total dissolved concentrations of Fe^{+2} and Na^+ after

acidification and dilution were made in 2 % nitric acid (final concentration in the diluted samples). Filtration (PALL® nylon membrane syringe filters with pore size of 0.2 μm) and acidification were performed inside the gloveboxes. Membrane filters with nitrate functional groups were not used to avoid oxidation of the ferrous iron upon contact. An Ion Chromatography (IC, DIONEX 3000) and a CO_2 coulometer (UIC, Inc., CM5015) were used to measure Cl^- and $EDTA^{-4}$, respectively.

Solids collected at the end of experiments were analyzed using an X-ray diffractometer (XRD, Bruker®, D8 Advance) in 2θ ranges of 10-90 degree. The X-ray tube was set at an acceleration voltage of 30 kV and a current of 30 mA. To avoid sample oxidation, solid was mounted on an anoxic sample holder inside the gloveboxes and the XRD scan was completed within 90 minutes or less from preparation of the mount. The solids were collected on 0.2 μm filters (PALL® nylon membrane filters). The solids were not rinsed with DDI water, with the goal of preserving all possible phases by not creating an abrupt undersaturation. The XRD scans were compared to Powder Diffraction Files (PDFs) contained in PDF-4+ 2018 (ICDD, International Centre for Diffraction Data).

RESULTS AND DISCUSSION

Solubility data are summarized in Table 1. Median values were used in thermodynamic model calculations for all components except the total dissolved concentrations of $EDTA^{-4}$ ($\sum EDTA^{-4}$); non-ignorable charge imbalance was observed, which could be attributed to the larger measurement error associated with the CO_2 coulometer. Thus, the charge imbalance divided by the absolute value of charge of $EDTA^{-4}$, i.e., (∑ positive charge - ∑ negative charge)/4, was added to the concentration of $\sum EDTA^{-4}$. The adjusted values for $\sum EDTA^{-4}$ are given in Table 2. The average of the seven adjusted values (0.041 molal) was used in the model calculation, and twice the standard deviation of the seven adjusted values (0.005 molal) is used as the error bars in Figures presented herein.

Figure 1 shows the XRD scans of solids harvested at the end of the experiments. Both ferrous iron hydroxide ($Fe(OH)_2$(s), FIH) and hibbingite ($Fe_2Cl(OH)_3$(s), HIBB) were observed in experiments with NaCl molality ≥ 0.75. With NaCl molality is less than 0.75, the solid is FIH.

Table 3 and Table 4 contain the 10-based logarithms of equilibrium constants (logKs) of the relevant reactions and the related Pitzer interaction parameters necessary to describe the solubility of FIH and HIBB in NaCl solutions in the presence of $EDTA^{-4}$. The acidity constants for EDTA acid (H_4EDTA, $C_{10}H_{16}O_8N_2$) were selected from Choppin et al. (2001).

The hydrolysis constants for Fe^{+2} and the dissolution constants for FIH and HIBB were taken from Kim et al. (2017). Four sets of the binary interaction parameters (i.e., $\beta^{(0)}$, $\beta^{(1)}$, $\beta^{(2)}$, and C^{ϕ}) for the four species pairs, i.e., Na^+/H_3EDTA^-, Na^+/H_2EDTA^{-2}, $Na^+/HEDTA^{-3}$, and $Na^+/EDTA^{-4}$ were referenced from Choppin et al. (2001).

An aqueous speciation code, EQ3NR packaged in EQ3/6, version 8.0a (Wolery, 2013), was used to determine speciation in Fe^{+2}-free aqueous NaCl solutions, in which the total dissolved concentration of

$EDTA^{-4}$ was set to 0.041 moles/kg of H_2O (Figure 2). $HEDTA^{-3}$ and $EDTA^{-4}$ are the major species, supporting that the Reaction (1) is of the concern.

Since FIH was observed in all seven experimental conditions (Figure 1), the $EDTA^{-4}$ speciation in Figure 2 was equilibrated with FIH to calculate the total dissolved molality of Fe^{+2} ($\sum Fe^{+2}$) at $\sum EDTA^{-4}$ = 0.041 (±0.005) moles/kg of H_2O (Figure 3). The calculated $\sum Fe^{+2}$ at lower NaCl molality with pmH < 8.5 is reciprocally changed with the NaCl molality because of the relatively high concentration of non-complexed species Fe^{+2} at pmH < 8.5 (blue line at the bottom of Figure 3), which is consistent with the initial drop of measured data for $\sum Fe^{+2}$. The calculated molality of $\sum Fe^{+2}$ at NaCl concentration of > 0.75 moles/kg of H_2O is independent of changes of pmH and NaCl concentration because Reaction (1) becomes dominant and $\sum EDTA^{-4}$ was set at 0.041 (±0.005) moles/kg of H_2O.

The Fe^{+2} activity is computed and plotted in the stability fields of FIH and HIBB in Figure 4. The boundary for FIH and HIBB (solid and dashed blue line in Figure 4) can be described by the equilibrium

$$Fe_2Cl(OH)_3(s)\ (HIBB) + H^+ = Fe(OH)_2(s)\ (FIH) + Fe^{+2} + Cl^- + H_2O, \qquad (2)$$

with logK = 4.19 (Table 3). The values for $\{Fe^{+2}\}$ at NaCl concentrations < 0.1 moles/kg of H_2O were in the stability field of FIH. At higher NaCl molalities FIH and HIBB coexisted (Figure 1).

IMPLICATION TO WIPP

It is hoped that aqueous Fe^{+2} can suppress the actinide - $EDTA^{-4}$ complexation by forming Fe^{+2} - $EDTA^{-4}$ complex. An exemplary calculation illustrates stronger complexation of Fe^{+2} with $EDTA^{-4}$ than Am^{+3} with the chosen $logK(FeEDTA^{-2})$ = -16.1 (Figure 5); when the Fe^{+2} - $EDTA^{-4}$ system above was equilibrated with a crystalline americium hydroxide, $Am(OH)_3$(cr), the species $FeEDTA^{-2}$ strongly suppresses the formation of $AmEDTA^-$. Solid orange line at the bottom of Figure 5 describes the concentration of $AmEDTA^-$ ($\approx \sum Am^{+3}$) in the presence of $Fe(OH)_2$(s), which would have been positioned at the location of $FeEDTA^{-2}$ in the absence of $Fe(OH)_2$(s). For the calculation in Figure 5, americium hydrolysis constants, chloride complexation constants, and dissolution constant for $Am(OH)_3$(cr) were selected from Guillaumont et al. (2003). Pitzer interactions parameters for the related Am^{+3} species and $logK(AmEDTA^-)$ = -18.97 for the reaction $AmEDTA^- = Am^{+3} + EDTA^{-4}$ are from Choppin et al. (2001). Discussion of the accuracy and consistency of the thermodynamic data for Am^{+3} used in this exemplary calculation would be beyond the scope of this study. However, given that the competition is sensitive to the accuracy of the rare thermodynamic data, such as, complexation constants for Fe^{+2} and Am^{+3}, this study warrants further investigation in the area.

ACKNOWLEDGMENT

Authors are grateful to Dr. Sungtae Kim and Shelly Nielsen for their reviews on this manuscript under Sandia National Laboratories' WIPP QA program. Data reproducibility and traceability much improved after their reviews. Dr. Charlotte Sisk-Scott put great effort to organize the laboratory activities to support this paper, which is much appreciated. Authors also thank Taya Olivas and Justin Dean for putting enormous efforts in maintaining the anoxic experiments for years. Sandia National Laboratories is a multi-mission laboratory managed and operated by National Technology and Engineering Solutions of Sandia, LLC., a wholly owned subsidiary of Honeywell International, Inc., for the U.S. Department of Energy's National Nuclear Security Administration under contract DE-NA-0003525. This research is funded by WIPP programs administered by the Office of Environmental Management (EM) of the U.S Department of Energy.

REFERENCES

Choppin, G. R., A. H. Bond, M. Borkowski, M. G. Bronikowski, J. F. Chen, S. Lis, J. Mizera, O. Pokrovsky, N. A. Wall, Y. -X. Xia, and R. Moore (2001). Waste Isolation Pilot Plant Actinide Source Term Test Program: Solubility Studies and Development of Modeling Parameters. Sandia Report, SAND99-0943, Sandia National Laboratories.

Guillaumont, R., T. Fanghänel, J. Fuger, I. Grenthe, V. Neck, D. A. Palmer, and M. H. Rand (2003) *Update on the chemical thermodynamics of uranium, neptunium, plutonium, americium and technetium*. Elsevier, Amsterdam.

Harvie, C. E., N. Møller, and J. H. Weare (1984) The prediction of mineral solubilities in natural waters: The Na - K - Mg - Ca - H - Cl - SO_4 - OH - HCO_3 - CO_3 - CO_2 - H_2O system to high ionic strengths at 25°C. *Geochimica et Cosmochimica Acta*, Vol. 48, 723-751.

Jang, J.-H. and S. Kim (2016) Derivation of Pitzer Interaction Parameters and Thermodynamic Properties for the Aqueous Species of Ferrous Iron and Their Pairs, revision 2; Sandia National Laboratories: Carlsbad, NM, U.S.A.

Kim, S., C. Marrs, M. Nemer, and J.J. Jang. (2017) Solubility model for ferrous iron hydroxide, hibbingite, siderite, and chukanovite in high saline solutions of sodium chloride, sodium sulfate, and sodium carbonate, *ACS Earth and Space Chemistry*, Vol. 1, 647-663.

Moog, H. C., Hagemann, S., and Rumyantsev, A. V., (2004) Isopiestic investigation of the systems $FeCl_2$-(Na, K, Mg, Ca)Cl_n-H_2O at 298.15 K. *Zeitschrift fur Physikalische Chemie - International Journal of Research in Physical Chemistry & Chemical Physics*, Vol. 218, 1063-1087.

Morel, F.M.M. and J.G. Hering (1993) Principles and applications of aquatic chemistry, John Wiley & Sons, Inc.

Pokrovsky, O. S., M. G. Bronikowski, R. C. Moore, and G. R. Choppin (1998) Interaction of Neptunyl(V) and Uranyl(VI) with EDTA in NaCl Media: Experimental Study and Pitzer Modeling. *Radiochimca Acta* Vol. 80, 23.

Shock, E.L., D. C. Sassani, M. Willis, and D. A. Sverjensky (1997) Inorganic species in geologic fluids: Correlations among standard molal thermodynamic properties of aqueous ions and hydroxide complexes. *Geochimica et Cosmochimica Acta*, Vol. 61, No. 5, 907-950.

Stumm, W. and J. J. Morgan (1996) Aquatic Chemistry, 3rd Edition, John Wiley and Sons.

Van Soest, G. D. (2012) Performance Assessment Inventory Report - 2012. Los Alamos National Laboratory Carlsbad Operations.

Wolery, T. J. (2013) Software Abstract, EQ3/6, A Software Package for Geochemical Modeling, Version 8.0a. Available as of August 2018 at, https://www-gs.llnl.gov/energy-cyber-and-infrastructure/geochemistry .

INSERTS: TABLES AND FIGURES

Table 1. Solubility data, in molality (m, mole solute in kg water), for $Fe(OH)_2(s)$and $Fe_2Cl(OH)_3(s)$ aged in NaCl + Na_2H_2EDTA solutions at ambient temperature and pressure.

Components	$\sum Na^+$	$\sum Cl^-$	$\sum Fe^{+2}$	$\sum EDTA^{-4}$	pmH
Exp. 1	9.44E-02, 9.27E-02	1.29E-02, 1.36E-02	5.29E-02, 4.99E-02	4.07E-02, 3.95E-02	7.79, 7.81
Median	**9.36E-02**	**1.33E-02**	**5.14E-02**	**4.01E-02**	**7.80**
Exp. 2	1.61E-01, 1.64E-01	8.15E-02, 8.33E-02	4.78E-02, 4.88E-02	3.96E-02, 4.02E-02	7.92, 7.89
Median	**1.62E-01**	**8.24E-02**	**4.83E-02**	**3.99E-02**	**7.91**
Exp. 3	8.26E-01, 8.44E-01	7.43E-01, 7.63E-01	3.89E-02, 3.98E-02	4.12E-02, 4.01E-02	8.35, 8.43
Median	**8.35E-01**	**7.53E-01**	**3.94E-02**	**4.07E-02**	**8.39**
Exp. 4	1.62E+00, 1.65E+00	1.54E+00, 1.57E+00	3.86E-02, 3.84E-02	4.12E-02, 4.06E-02	8.82, 8.72
Median	**1.64E+00**	**1.56E+00**	**3.85E-02**	**4.09E-02**	**8.77**
Exp. 5	2.48E+00, 2.31E+00	2.39E+00, 2.23E+00	3.86E-02, 3.77E-02	4.31E-02, 4.14E-02	9.10, 9.08
Median	**2.40E+00**	**2.31E+00**	**3.82E-02**	**4.22E-02**	**9.09**
Exp. 6	2.89E+00, 3.17E+00	2.81E+00, 3.09E+00	3.44E-02, 3.67E-02	4.12E-02, 4.18E-02	9.21, 9.33
Median	**3.03E+00**	**2.95E+00**	**3.56E-02**	**4.15E-02**	**9.27**
Exp. 7	3.64E+00, 3.45E+00	3.56E+00, 3.36E+00	3.64E-02, 3.53E-02	4.31E-02, 4.28E-02	9.48, 9.45
Median	**3.55E+00**	**3.46E+00**	**3.59E-02**	**4.29E-02**	**9.47**

Experiments were sampled at 500 and 1000 days since the preparations.

Table 2. Adjusted total dissolved molalities of $EDTA^{-4}$ ($\sum EDTA^{-4}$) with respect to the charge imbalance noticed from the data in Table 1. The average $\sum EDTA^{-4}$ molality after the charge correction is 0.041 molal with twice the standard deviation of 0.005 molal (12 %).

$\sum EDTA^{-4}$ (before charge correction)	$\sum$ positive charge	$\sum$ negative charge	($\sum$ positive charge - $\sum$negative charge)/4	$\sum EDTA^{-4}$ (after charge correction)
4.01E-02	0.196	0.174	5.64E-03	4.58E-02
3.99E-02	0.260	0.242	4.38E-03	4.43E-02
4.07E-02	0.914	0.916	-5.51E-04	4.01E-02
4.09E-02	1.717	1.720	-6.73E-04	4.02E-02
4.22E-02	2.476	2.480	-9.05E-04	4.13E-02
4.15E-02	3.101	3.116	-3.70E-03	3.78E-02
4.29E-02	3.622	3.632	-2.47E-03	4.05E-02

Figure 1. XRD scans of $Fe(OH)_2(s)$ and $Fe_2Cl(OH)_3$ aged for up to 1000 days in NaCl + Na_2H_2EDTA solutions. No $EDTA^{-4}$ - containing solid was observed in any samples. $Fe(OH)_2(s)$ and $Fe_2Cl(OH)_3(s)$ coexisted in experiments with NaCl ≥ 0.75 m.

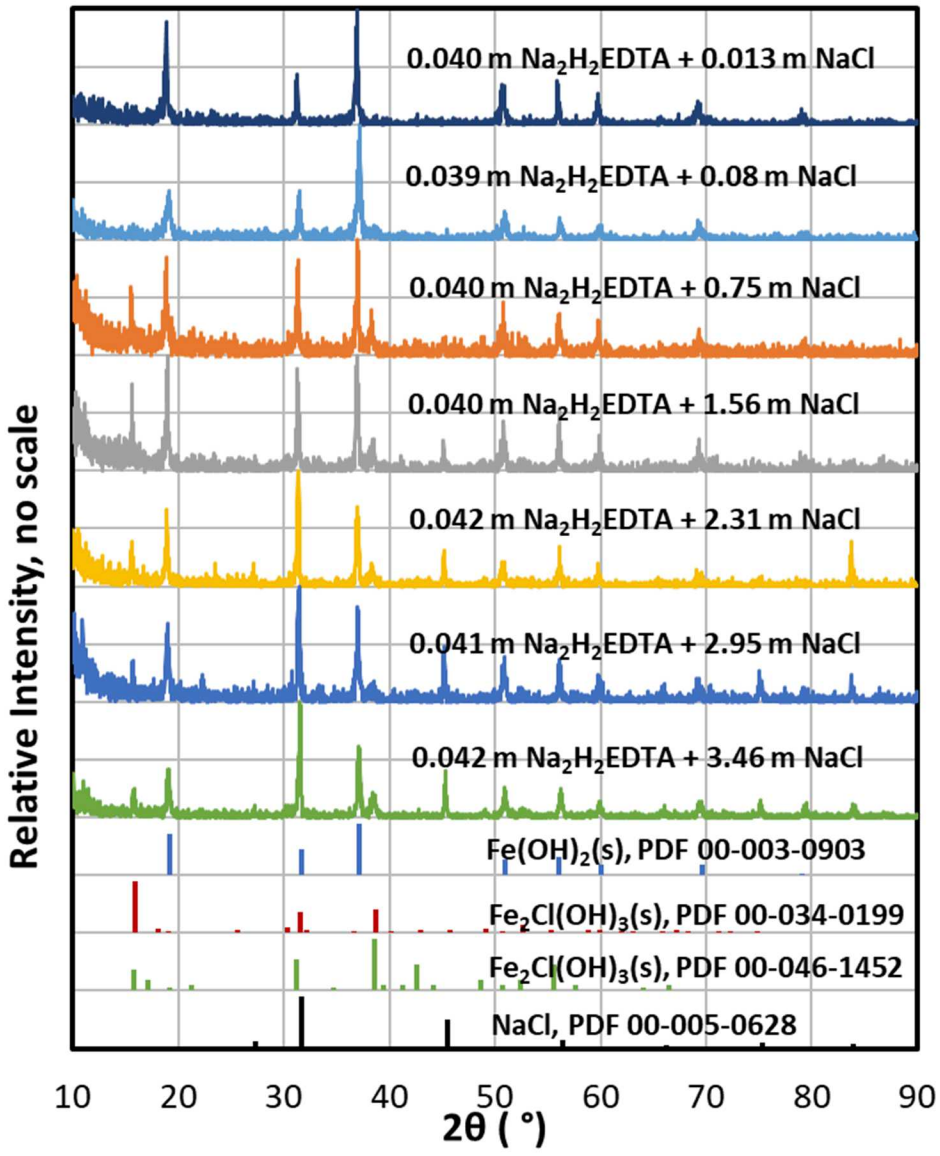


Table 3. Reactions and 10-based logarithms of their equilibrium constants for the Fe^{+2} - Na^{+} - H^{+} - Cl^{-} - $EDTA^{-4}$ - H_2O system at infinite dilution at 25 °C and 1 atm.

Reactions	LogK	Source
Aqueous reactions		
$H^+ + OH^- = H_2O$	13.99	Harvie et al. (1984)
$H_4EDTA(aq) = 4H^+ + EDTA^{-4}$ [A]	-23.03	Choppin et al. (2001)
$H_3EDTA^- = 3H^+ + EDTA^{-4}$	-20.53	Choppin et al. (2001)
$H_2EDTA^{-2} = 2H^+ + EDTA^{-4}$	-17.45	Choppin et al. (2001)
$HEDTA^{-3} = H^+ + EDTA^{-4}$	-10.57	Choppin et al. (2001)
$FeEDTA^{-2} = Fe^{+2} + EDTA^{-4}$	-16.1	Morel and Hering (1993)
$FeOH^+ + H^+ = Fe^{+2} + H_2O$	9.31	Shock et al. (1997)
$Fe(OH)_2(aq) + 2H^+ = Fe^{+2} + 2H_2O$	20.82	Stumm and Morgan (1996)
Dissolution		
$Fe(OH)_2(s) + 2H^+ = Fe^{+2} + 2H_2O$	12.89[A]	Kim et al. (2017)
$Fe_2Cl(OH)_3(s) + 3H^+ = 2Fe^{+2} + Cl^- + 3H_2O$	17.08[A]	Kim et al. (2017)

[A] At ambient temperature and pressure

Table 4. Pitzer interaction parameters for the Fe^{+2} - Na^{+} - H^{+} - Cl^{-} - $EDTA^{-4}$ - H_2O system at 25 °C and 1 atm.

i	*j*	α_1/α_2[A]	$\beta^{(0)}$	$\beta^{(1)}$	$\beta^{(2)}$	C^{Φ}	Source
Na^+	Cl^-	2.0/12.0	0.0765	0.2664	0.0	0.00127	Harvie et al. (1984)
Na^+	OH^-	2.0/12.0	0.0864	0.253	0.0	0.0044	Harvie et al. (1984)
Na^+	H_3EDTA^-	2.0/12.0	-0.2345	0.29	0.0	0.059	Choppin et al. (2001)
Na^+	H_2EDTA^{-2}	2.0/12.0	-0.1262	1.74	0.0	0.054	Choppin et al. (2001)
Na^+	$HEDTA^{-3}$	2.0/12.0	0.5458	5.22	0.0	-0.048	Choppin et al. (2001)
Na^+	$EDTA^{-4,}$	2.0/12.0	1.016	11.6	0.0	0.001	Choppin et al. (2001)
H^+	Cl^-	2.0/12.0	0.1775	0.2945	0.0	0.0008	Harvie et al. (1984)
Fe^{2+}	Cl^-	2.0/12.0	0.37324	1.13499	0.0	-0.02152	Moog et al. (2004)
i	***j***	θ_{ij}	**Source**		***k***	ψ_{ijk}	**Source**
Na^+	H^+	0.036	Harvie et al. (1984)		Cl^-	-0.004	Harvie et al. (1984)
Cl-	OH^-	-0.05	Harvie et al. (1984)		Na^+	-0.006	Harvie et al. (1984)
Na^+	Fe^{2+}	0.10945	Moog et al. (2004)		Cl^-	-0.01605	Moog et al. (2004)

[A] α_1 and α_2 are pre-set constants used in the Pitzer activity coefficient equation. α_1 and α_2 apply for only cation-anion binary pair. α_2 is not applied when $\beta^{(2)}$ is zero or not used. Unit for α_1 and α_2 is $kg^{1/2} \cdot mol^{-1/2}$.

Figure 2. Speciation of $EDTA^{-4}$ in NaCl solutions in the absence of Fe^{+2}. $\sum EDTA^{-4}$ = 0.041 molal. Species of less relevance are not shown for clarity.

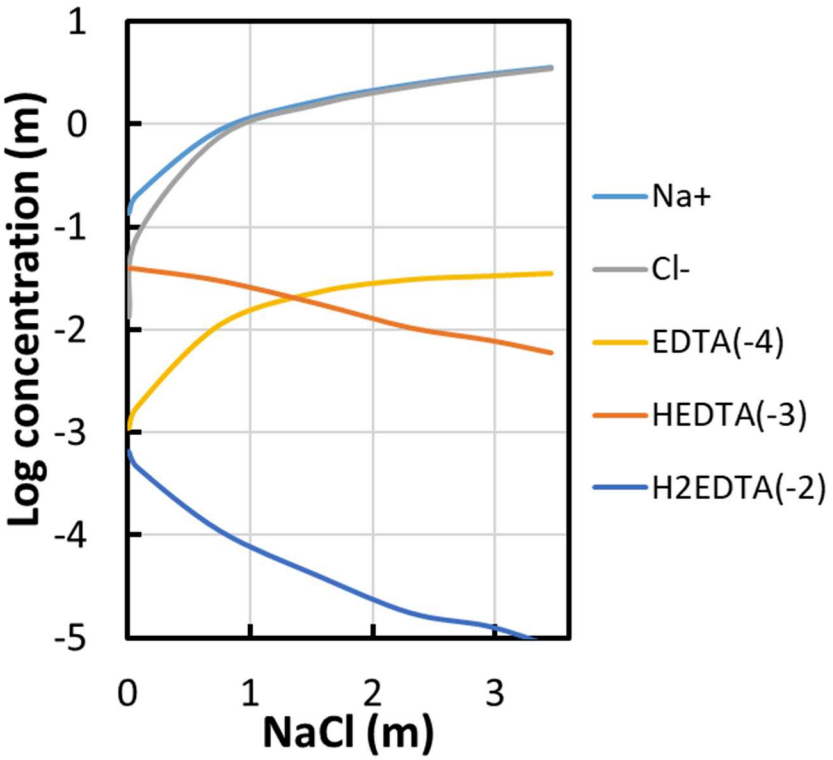


Figure 3. Calculated total dissolved concentration of Fe^{+2} ($\sum Fe^{+2} = Fe^{+2} + FeEDTA^{-2}$) using the logKs and Pitzer interaction parameters in Table 3 and Table 4. Species of molalities less than 10^{-4} are not shown.

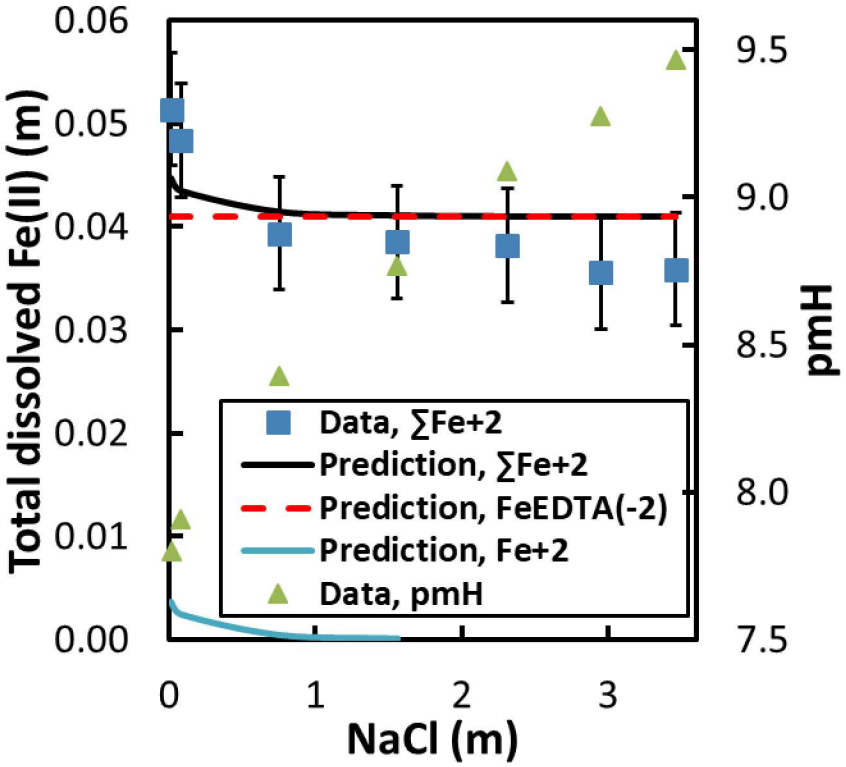


Figure 4. Stability fields of $Fe(OH)_2(s)$ and $Fe_2Cl(OH)_3(s)$ at NaCl = 0.013 to 3.46 molal, pmH = 7.8 to 9.4. The blue solid line is the boundary of FIH and HIBB given by Reaction (2). The blue dashed line is the metastable extension of the boundary. The calculated log{Fe^{+2}} for the five highest NaCl molalities delineates the coexistence of FIH and HIBB (solid blue line), consistent with the XRD results. The two lowest NaCl molality data and solid black line delineates the equilibrium solubility of FIH.

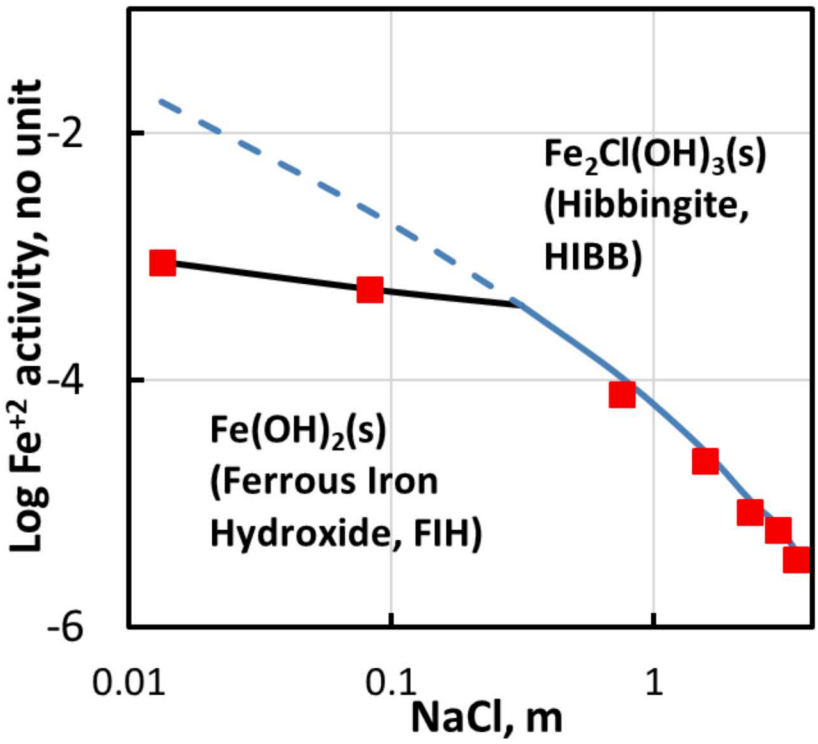


Figure 5. Solubility of $Fe(OH)_2(s)$ and $Am(OH)_3(s)$ in NaCl solutions in the presence of 0.041 molal $\sum EDTA^{-4}$. Total dissolved Am^{+3} concentration ($\sum Am^{+3}$, the same as $[AmEDTA^-]$, orange line below) in the presence of $Fe(OH)_2(s)$ under the same experimental conditions, i.e., $\sum EDTA^{-4}$ = 0.041 molal and calculated total ionic strength = 0.14 to 3.6 molal. $FeEDTA^{-2}$ effectively suppresses the formation of $AmEDTA^-$.

